Opuscula Mathematica • Vol. 24/1 • 2004

Piotr Schulz

INSTABILITY AND THE FORMATION OF BUBBLES AND THE PLUGS IN FLUIDIZED BEDS

Abstract. This is an review paper, particulary concentrate on results not many researches by reason that are explain in the text. We consider stability of disperse, two-phase flow (gas-solid particles or liquid-solid particles) linear and non-linear. In particular we discuss the result of Anderson, Sundareson and Jackson (1995) [3] that for vertical dispersion flow one- and two-dimensional, they attack problem growing disturbances directly by numerical integration of equations of motion from given initial conditions (using computer Cray C-90). In principle, this would allow authors to explore all aspects of dynamical behaviour of fluidized beds. It is interesting mechanism of periodic plug describing by Anderson *et al.* and attest by other researchers. Second part of paper is more general, dedicate the problem of linear stability of uniformly fluidized state ("fluidized bed"). We make the most important stages of calculations (after to Jackson (2000) [23]) and demonstrate that the majority (but not all) of fluidized beds with parameters having technical importance is unstable, or stable in narrow interval of wave numbers k.

Keywords: multiphase flow, bubbling, linear and non linear instability, dispersion relation, periodic plugs (or slugs).

Mathematics Subject Classification: 76-02, 76E30, 76M10, 76T10, 76T20.

1. INTRODUCTION

The occurrence of multiphase flows is very widespread. Indeed, vapor/liquid flows are common in power production and utilization technologies and in chemical processing. Likewise, solid/fluidal slurry flows, fluidized beds and various combustion processes are other common examples of important multiphase flows.

Fluidized beds are used extensively in industry for processes such as catalytic reactions, which require a good contact area between a fluid and a solid. Particles with diameters ranging froms 10^{-2} to 1 mm are normally used, and these rest on each other on porous plate in vertical tube. Fluid is pumped upward through the system

and on incrising the fluid flow speed a point is reached where the upward drag exerted by the fluid balances the downward gravitational force on the particles, which then become buoyant. At this point the bed is fluidized at minimum fluidizing velocity exhibiting large-scale phenomena, such as buoyancy and surface waves; similar to those of liquid.

In gas-fluidized beds, it is possible for uniform expansion to occur over a small range of gas velocities, but at higher flow rates the bed becomes unstable and some of the fluid passes through the bed in the form of bubbles or slugs. Bubbling occurs in the beds whos diameters are large compared with their height and is characterized by approximately spherical high-voidage regions propagating upwards through the bed, while slugging is formed in narrow-diameter beds and is characterized by horizontal bands of high voidage propagating upwards through the bed. And as well clusters as compact regions of high particle concentration.

This behaviour (bubbles) can also occur in liquid-fluidized beds when the ratio of the density of the solid to that of the liquid is high (e.g. lead shot fluidized with water). In most liquid-fluidized beds, however, although instability is present and can be seen in the form of wavy structures this does not lead rapidly to bubble formation. There are two sorts of slugging, both of which are strongly influenced by the container walls. In the first type, highly deformed bubbles (whose frontal diameters are equal the size of the tube rise slowly and displace particles, which flow down at the sides. In the second type, which is common in tubes up to 4–5 cm in the diameter we have slowly rising bands of particle-deficient regions, with rapid particle raining occurring at the interfaces.

Since bubbling und slugging are often undesirable for efficient operation, many theoretical studies have been aimed at describing and understanding the mechanisms involved in the development of such phenomena. Therefore, much interst has been shown in the mathematical modelling of such system in order to try and understand the mechanism governing instability. A popular approach, which we shall adopt here, used by Jackson (1963 a,b) [21, 22], Murray (1965)[31], Pritchett (1975) [32], Needham & Merkin (1986) [33] et others, is that of interacting continua.

The point variables are averaged over a volume which is small compared to the whole system, but is large compared to the particle size and spacing. This yields continuum equations for the particles and fluids, which are then treated as two interpenetrating one-phase fluids. Many autors have all carried out linear instability analysis of small disturbances superimposed on a uniformly fluidized bed. Jackson (1963) [33,22] find the bed to be unstable in all cases. This disagrees with observations and Garg and Pritchett (1975) [12] show the importance of including a 'particle pressure' which has stabilizing influence.

By a suitable choice of the particle pressure as a function of solids volume fraction it was possible to explain the stability of fluidized beds. However, the resulting is not predictive in the absence of a method of calculating the particle pressure from first principles.

Batchelor (1988) [4] suggested that the particle pressure be related to the hydrodynamic particle self-diffusivity in a low Reynols number liquid-solid suspension and used measurements and plausible reasoning concerning this quantity to suggest a model for particle pressure.

While this suggestion has some physical basis, it ignores inertial effects and is applicable to low-to-moderate Reynolds number-fluidized beds.

The linear instability does not guarantee that the perturbation will grow into well-formed bubbles or slugs, as once the perturbation amplitude is large, enough nonlinear effects must be taken into account, while further linear mechanism also come into play, and tend themselves to disperse voidage concentrations.

Experiments Anderson & Jackson (1969) [2]; El-Kaissy & Homsy (1976) [8] show that liquid-fluidized bed of small glass beads which are typically 'particulate' on behaviour, are not uniform and stable but are traversed by slowly developing rising waves closely resembling in their initial. Stages of growth, the instability waves closely resembling in their initial. A theoretical prediction of stability in these cases would therefore, be unwelcome.

The physical origin of such a stabilizing term has been the subject of much debate (Gibilaro (1984), Batchelor (1988) [4] for example).

A few studies have examined nonlinear effects, although the inclusion of the nonlinear terms presents a severe impediment to analysis.

Over the intervening years there have been a number of attempt to extend the one-dimensional stability theory to take account of the nonlinearity of the equation of motion Liu (1982) [30]; Needham & Merkin (1986) [33], Ganser & Drew (1990) [11] but these have failed to show any qualitative distinction between the predicted behaviour of gas — and liquid – fluidized beds and recent bifurcation analyses, again confined to one-dimensional motion (Göz 1992) [17] also show no significant differences between the two cases.

Secondary, two-dimensional instabilities of the one-dimensional wave pattern have been observed experimentally in water-fluidized beds (Didwania & Homsy (1981) at investigated theoretically by the same authors (Didwania & Homsy (1982)), and by Needham & Merkin (1986), and Batchelor (1993). These appear to play a role in a process that may lead to bubbles, but again the stability analyses are not able to predict the distinction in behaviour between gas-and liquid-fluidized beds.

The direct numerical integration of the motion equation had served as a basis for the stability analyses, propagating, bubble-like structures in fluidized beds were found as early as 1978 Pritchett *et al*, Hu, Crochet & Joseph, (1991) [20] Anderson *et al.* (1995) [3] Saurel, Lemetayer, (2001) [35] (unconditionally hyperbolic model); Kolev (2002) [28].

In this paper we try to present in outline:

a) The linear stability analysis of uniformly fluidized state, deriving the full dispersion relations for propagation density waves of small amplitude and examining the conditions under which they growth or decay.

b) The results of Anderson *et al.* (1995) [3] for the particular case of a bed of 200 μm diameter glass fluidized by air and 1 mm fluidized by water; obtain by direct integration equations of motion, the case one-dimensional.

c) The numerical results of Anderson *et al.* (1995) [3] and Glasser *et al.* (1997) [15] (bifurcation theory) confirm the hypothesis putting forward by Schulz (1979) [36] and (1985a) [37], that in ventilation shaft of mine suspension of water drops form periodic plugs (or slugs) unstable.

2. EQUATIONS OF MOTION

Ensamble-averaged (or time averaged, volume-time averaged) equations of motion for the fluid and particle phases in fluid-particle suspensions have been described extensively in the literature, for example, see Anderson & Jackson (1967) [1]; Garg & Pritchett (1975) [11]; Nigmatulin (1979) [33]; Drew & Lahey (1993) [6]; Joseph & Lundgren (1993) [25]; Zhang & Prosperetti [38]; Anderson *et al.* (1995) [3]; Kolev (2002) [27].

Averaged equations have been explicitly or implicitly used by many of previous researchers to model the flow in fluidized beds. The equations used in this work are those proposed by Anderson & Jackson (1967) [1].

Assuming an incompresible fluid and defining the following average variables: $\mathbf{v}$ the solids velocity, $\mathbf{u}$ the fluid velocity,ϕ the volume fraction of the solids particles, $\boldsymbol{\sigma}_s$ the solid-phase stress tensor, $\boldsymbol{\sigma}_f$ the fluid phase stress tensor, the equations of continuity and motion for the solid and fluid phases are

$$\frac{\partial \phi}{\partial t} + \nabla \cdot (\phi \mathbf{v}) = 0 \tag{1}$$

$$\frac{\partial (1-\phi)}{\partial t} + \nabla \cdot \Big((1-\phi)\, \mathbf{u} \Big) = 0 \tag{2}$$

$$\rho_s \phi \frac{D_s \mathbf{v}}{Dt} = -\nabla \cdot \boldsymbol{\sigma}_s + \mathbf{F} + \phi(\rho_s - \rho_f)\mathbf{g} + \rho_f \phi \frac{D_f \mathbf{u}}{Dt} \tag{3}$$

$$\rho_f \phi \frac{D_f \mathbf{u}}{Dt} = -\nabla \cdot \boldsymbol{\sigma}_f - \mathbf{F} + \rho_f \mathbf{g} \tag{4}$$

ρ_f and ρ_s are densities at the fluid and solid materials, $\mathbf{g}$ is specific gravity force vector. $\mathbf{F}$ is average drag force, per unit bed volume exerted on particle by the fluid due to the relative velocity of the phases. $\boldsymbol{\sigma}_f$ and $\boldsymbol{\sigma}_s$ are stress tensors associated with the separate momentum balances. The symbol $\frac{D_f}{Dt}$ and $\frac{D_s}{Dt}$ denote material the derivatives based on velocities $\mathbf{u}$ and $\mathbf{v}$, respectively:

$$\frac{D_s}{Dt} = \frac{\partial}{\partial t} + \mathbf{v} \cdot \nabla \quad \frac{D_f}{Dt} = \frac{\partial}{\partial t} + \mathbf{u} \cdot \nabla.$$

In the present study a Newtonian form is assumed for the fluid and solid-phase stress tensors.

$$\boldsymbol{\sigma}_s = p_s \mathbf{I} - \mu_s \Big[\nabla \mathbf{v} + (\nabla \mathbf{v})^T - \frac{2}{3} (\nabla \cdot \mathbf{v}) I \Big] \tag{5}$$

$$\boldsymbol{\sigma}_f = p_s\mathbf{I} - \overline{\mu}_f\Big[\nabla\mathbf{u} + (\nabla\mathbf{u})^T - \frac{2}{3}(\nabla\cdot\mathbf{u})I\Big] \tag{6}$$

and the drag force

$$\mathbf{F} = \beta(\mathbf{u}-\mathbf{v}) \tag{7}$$

proportional to the difference between the local average velocities and $\beta = \beta(\phi)$.

The particle-phase pressure, p_s, and effective particle-phase viscosity, μ_s, need to be determined empirically or from modelling consideration. $\overline{\mu}_f$, the effective viscosity of the fluid, was assumed to equal $\overline{\mu}_f$, the viscosity of the fluid itself. The fluid pressure, p_f, is determined dynamically since we have assumed the fluid to be incompressible. For the moment the precise forms for p_s and μ_s are not crucial for our analysis so we take $p_s(\phi)$ and $\mu_s(\phi)$ monotonically increasing function of ϕ when $\phi \to \phi_p$, where ϕ_p is volume fraction of solids at random close packing of the particles.

We presume that $p_s(0) = 0$, $\mu_s(0) = 0$. Since the functional form of p_s and μ_s is still a subjects of debate Anderson *et al.* adopted a functions:

$$p_s = p\phi^3 \exp\left(\frac{r\phi}{\phi_p - \phi}\right) \tag{8}$$

and

$$\mu_s = \frac{M\phi}{1-(\phi/\phi_p)^{1/3}} \tag{9}$$

One can take it more simple forms:

$$p_s = \frac{p\phi}{\phi_{cp}-\phi} \quad \text{and} \quad \mu = \text{const} \tag{10}$$

ϕ_{cp} is the random close packing volume fraction of solids. Function $p_s(\phi)$ represent a (average) particle phase pressure which increases from zero when $\phi = 0$ and diverges as the solids fraction tends to the random close-packed value, ϕ_p.

If $p_s(\phi) \equiv 0$ — the fluidized bed is unstable. The p_s closures analyzed in many previous studies (Foscolo & Gibilaro (1987) [10]; Batchelor (1988) [4]; Koch & Sagani (1999) [26] reduce to a linear variation of p_s with ϕ as $\phi \to 0$. See e.g. Figure 2.

If we had been interested only in gas-fluidized beds we could have gone further and introduced approximations associated with the smolness of the density of the density and viscosity of the density and viscosity of typical gas, when equations (3) and (4) above would reduce to

$$\rho_s\phi\frac{D_s\mathrm{v}}{Dt} = -\nabla\cdot(\boldsymbol{\sigma}_s + p_f I) + \rho_s\phi\mathbf{g} \tag{11}$$

and

$$\beta(\phi)(\mathbf{u}-\mathbf{v}) = -\nabla p_f \tag{12}$$

3. CLOSURE CONDITIONS

The general three dimensional, unsteady, two-phase (multiphase) model given by (1)–(4) and (5)–(9) must be supplemented with state equations, constitutive equations in case the nonnewtonianflows, and boundary and initial conditions.

The general problem of closure for equations (1)–(9) is to provide expressions for the tensors $\boldsymbol{\sigma}_f$ and $\boldsymbol{\sigma}_s$ and the vector $\mathbf{F}$ that are applicable over the whole range of Reynolds and Stokes numbers and up to high values of particle volume fraction ϕ. On define:

Reynolds number: $$Re = \frac{a\rho_f v_2}{\mu}$$

Stokes number: $$St = \frac{a\rho_s v_1}{\mu}$$

where v_2 is average relative velocity of the particles and the fluid is their neighborhood, and if Re is small compared to unity, inertia associated with the motion of the fluid around and between the particles can be neglected. In gas fluidized bed this Reynolds number is typically of the order unity (linear theory). In the solutions for the liquid-fluidized bed, on other hand Reynolds numbers a decimal order of magnitude larger then this are typical and linear form (7) should be replaced by something more elaborate. v_1 — is the relative velocity of approach of pair of particles. Stokes number represents relative averaged interactions between the fluid and particles, and those representing contact forces between particles.

The drag force per unit volume F is dependent non only of reciprocal motion of fluid and particles but as well as on boundary and initial conditions.

Let as present the drag force F in form $\mathbf{F} = n\mathbf{f}$ where n is Richardson & Zaki (1954) coefficient (exponens). It is generally agreed that the main contributions this force are a term depending on particle concentration and the relative velocity $(\mathbf{u}-\mathbf{v})$, a second term depending on the concentration, and the third term representing a force normal to the direction $(\mathbf{u}-\mathbf{v})$. These are referred to as the drag force F_D, the virtual mass force $\mathrm{F_v}$, and the lift force F_L, respectively. Other contributions usually neglected, include the Faxen force and a history-dependent term — a comprehensive listing is given by Drew & Lahey (1993) [6], Gidaspow (1994) [13] and Kolev (2002) [27].

We can write

$$\mathbf{F} = n\mathbf{f} = \mathbf{F}_D + \mathbf{F}_V + \mathbf{F}_L \tag{13}$$

and discuss separately every contributions.

The drag force acts in the direction of relative velocity $(\mathbf{u}-\mathbf{v})$ and therefore has the general form $\mathbf{F}_D = (\mathbf{u}-\mathrm{v})F(\phi, |\mathbf{u}-\mathrm{v}|)$ where the form of the scalar function F is to be determined and will dependend on the particle size and shape and the properties of the fluid in addition to arguments indicated. The experimental information with most direct bearing on the form of $\mathbf{F}_D$ is the observed relation between the sedimentation velocity v_s of a dispersion of the particles in the fluid and their concentration,

measured by ε. This was investigated extensively by Richardson & Zaki (1954), who found the following empirical relation for a suspension of uniform, spherical particles, infinite in extent:

$$v_s = v_t \varepsilon^n \tag{14}$$

with

$$n = \begin{cases} 4.65 & & for & Re_t < 0.2 \\ 4.35 & Re_t^{-0.03} & for & 0.2 < Re_t < 1 \\ 4.45 & Re_t^{-0.1} & for & 1 < Re_t < 500 \\ 2.39 & & for & 500 < Re_t \end{cases} \tag{15}$$

The force F_D is usually correlated to the Reynolds number $Re_t := 2a\rho_f \dfrac{v_t}{\mu}$ for isolated particle at is terminal velocity of fall under gravity, v_t in the fluid.

Typical values of numbers Re and St for fluidized beds are done in Appendix.

The relation (14) is sufficient to determine the functional form for F_D completely at both small and large values of $|\mathbf{u}-\mathbf{v}|$. For small values of $|\mathbf{u}-\mathbf{v}|$, F_D is proportional to the relative velocity so we can write

$$\mathbf{F}_D = \beta(\mathbf{u} - \mathbf{v}).$$

Applying this to the case of steady sedimentation, where $\boldsymbol{\sigma}_s = 0$ and $\boldsymbol{\sigma}_f = -\rho_f \mathbf{I}$ reduces equations (3) and (4) to

$$0 = -\varepsilon \frac{dp_f}{dz} - \beta(u - v) - \rho_f \varepsilon g,$$
$$0 = -\phi \frac{dp_f}{dz} + \beta(u - v) - \rho_f \phi g,$$

where z is a coordinate in the upward direction, u and v are the z components of $\mathbf{u}$ and $\mathbf{v}$, respectively. Since the total volume flux vanishes, $\varepsilon u + \phi v = 0$ and it is possible determine coefficient β, and the force F_D:

$$\beta = \frac{(\rho_s - \rho_f)\phi g}{v_t \varepsilon^{n-2}}, \qquad \mathbf{F}_D = \frac{(\rho_s - \rho_t)\phi g}{v_t \varepsilon^{n-2}}(\mathbf{u} - \mathbf{v}) \tag{16}$$

with n determined from (15).

If the value of $|\mathbf{u} - \mathbf{v}|$ is sufficiently large the regime of fluid flow relative to the particles is Newtonian, so we can expect that

$$\mathbf{F}_D = \alpha(\mathbf{u} - \mathbf{v})|\mathbf{u} - \mathbf{v}| \tag{17}$$

Than we can easily found:

$$\alpha = \frac{(\rho_s - \rho_f)\phi g}{v_t^2 \varepsilon^{2n-3}}, \quad \mathbf{F}_D = \frac{(\rho_s - \rho_f)\phi g}{v_t^2 \varepsilon^{2n-3}}(\mathbf{u} - \mathbf{v})|\mathbf{u} - \mathbf{v}| \tag{18}$$

For values of the relative velocity intermediate between the viscous and Newtonian regimes a factorization of this sort is not possible.

The virtual mass force is the force exerted on the moving object when it accelerates through a fluid. If an object is immersed in fluid and accelerated, it must accelerate some of the surrounding fluid. This results in an interaction force on the object.

A suitable form for $\mathrm{F_v}$ is suggested by the exact expression derived by Zhang & Prosperetti (1994) [38] for an inviscid fluid at the limit of low particle concentration, namely

$$\mathbf{F}_{\mathrm{v}} = \frac{1}{2}\rho_f \phi \left(\frac{D_f \mathbf{u}}{Dt} - \frac{D_s \mathbf{v}}{Dt} \right) \tag{19}$$

At higher values of ϕ coefficient $\frac{1}{2}$ this should presumably be replaced by $c_{\mathrm{v}}(\phi)$; where $c_{\mathrm{v}}(\phi)$ is concentration-dependent virtual mass coefficient. Zuber (1964) has proposed simple formula:

$$c_{\mathrm{v}}(\phi) = \frac{1}{2} + \frac{3}{2}\phi$$

at moderate values of ϕ. For a single particle it is $c_{\mathrm{v}} = \frac{1}{2}$. The general, precise formula for $\mathrm{F_v}$ is not known.

If a particle moves through a fluid that is in shearing motion then the particle experiences a force transverse to the direction of motion.

Such a force is often called a 'lift force'.

If the particle is spherical, the force is given by Drew & Lahey (1993) [6] for an inviscid fluid as

$$\mathbf{F}_L = c_L(\phi)\rho_f \rho_s \phi (\nabla \times u) \times (\mathbf{v} - \mathbf{u}) \tag{20}$$

with

$$c_L \to \frac{1}{2} \quad \text{when} \quad \phi \to 0$$

4. SMALL PERTURBATIONS UNIFORMLY FLUIDIZED STATE. LINEAR ANALYSIS

In this chapter we shall confine our attention to linear stability analysis of uniformly fluidized state deriving in outline the full dispersion relations for propagating density waves of small amplitude and examining conditions under which they grow and decay. Linear stability have been investigated for a long time by Needham & Merkin (1986) [33]; Foscolo & Gibilaro (1987) [10]; Lammers & Bieheuvel (1996) [20]; Göz (1992) [17]; Koch & Sangani (1999) [26]; et other cited in introduction. We make a summary the paper of Jackson (2000) [23]; pp. 99–153. Jackson study the pure hydrodynamic problem (i.e. without any chemical reaction etc.); physicaly this is a uniformly fluidized suspension of infinite extent in R^3 with the particles suspended at rest by an upward flow of fluid sufficient to provide a drag force that exactly

balances their buoyant weight. In particular we shall examine the stability of this solutions against small perturbations (using conventional linear analysis). To do this we must, of course have explicit form for the equation of motion. For the continuity equation we have:

$$\frac{\partial(1-\phi)}{\partial t} + \nabla \cdot ((1-\phi)\mathbf{u}) = 0 \quad \text{(fluid)} \tag{21}$$

and

$$\frac{\partial \phi}{\partial t} + \nabla \cdot (\phi \mathbf{v}) = 0 \quad \text{(particles)} \tag{22}$$

The equations of motion for the solid and fluid phase are (5) and (6). For drag force we take the form (16) which is appropriate for small values of a Reynolds number based on the particle diameter and the slip velocity. Lift force is neglected.

Then

$$n\mathbf{f} = \beta(\phi)(\mathbf{u}-\mathbf{v}) + \frac{\rho_f \phi c_v}{1-\phi}\left(\frac{D_f \mathbf{u}}{Dt} - \frac{D_s \mathbf{v}}{Dt}\right) \tag{23}$$

where n is the Richardson–Zaki exponent (see (14)). Thus, the momentum equations take the following explicit form:

$$\rho_f \frac{D_f \mathbf{u}}{Dt} = -\beta(\mathbf{u}-\mathbf{v}) - \frac{\rho_f \phi c_v}{1-\phi}\left(\frac{D_f \mathbf{u}}{Dt} - \frac{D_s \mathbf{v}}{Dt}\right) + \rho_f \mathbf{g} - \nabla p^f + \\ + \nabla \cdot \left\{\mu_f(\nabla \mathbf{u} + (\nabla \mathbf{u})^T - \frac{2}{3}(\nabla \cdot \mathbf{u})\mathbf{I})\right\} \quad \text{(fluid)} \tag{24}$$

$$\rho_s \phi \frac{D\mathbf{v}}{Dt} = \beta(\mathbf{u}-\mathbf{v}) + \frac{\rho_f \phi c_v}{1-\phi}\left(\frac{D_f \mathbf{u}}{Dt} - \frac{D_s \mathbf{v}}{Dt}\right) + (\rho_s - \rho_f)\phi \mathbf{g} + \\ + \rho_f \phi \frac{D_f \mathbf{u}}{Dt} - \nabla p_s + \nabla \cdot \left\{\mu_s(\nabla \mathbf{v} + (\nabla \mathbf{v})^T - \frac{2}{3}(\nabla \cdot \mathbf{v})\mathbf{I})\right\} \quad \text{(particles)} \tag{25}$$

As basic state we denote that stability and homogenous (uniformly) solution of eq. (21)–(25), for which the particles do not move, while the fluid is moving with constant velocity against the direction of gravity.

We are examined the linear stability uniformly suspension with $\mathbf{u} = \mathbf{u}_0 = \mathbf{i}u_0$ and $\mathbf{v} = \mathbf{0}$ where $\mathbf{i}$ denotes the unit vector in the upward vertical direction. In this state the equations (24) et (25) reduce to

$$\beta(\phi_0)u_0 + \rho_f g + \frac{dp_0^f}{dx} = 0 \tag{26}$$

and

$$\beta(\phi_0)u_0 - (\rho_s + \rho_f)\phi_0 g = 0 \tag{27}$$

where x is coordinate measured vertically upward.

This uniform state is perturbed slightly, writing $\mathbf{u} = \mathbf{i}u_0 + \mathbf{u}_1$, $\mathbf{v} = \mathbf{v}_1$ and $p^f = p_0^f + p_1^f$, and the equations are linearized in the perturbations, giving

$$-\frac{\partial \phi_1}{\partial t} + (1-\phi_0)\nabla \cdot \mathbf{u}_1 - \mathbf{u}_0 \frac{\partial \phi_1}{\partial x} = 0 \tag{28}$$

$$\frac{\partial \phi_1}{\partial t} + \phi_0 \nabla \cdot \mathbf{v}_1 = 0 \tag{29}$$

$$\begin{aligned}\left[\rho_f + \frac{\rho_f \phi_0 c_v}{1-\phi_0}\right]\left(\frac{\partial \mathbf{u}_1}{\partial t} + u_0 \frac{\partial \mathbf{u}_1}{\partial x}\right) - \frac{\rho_f \phi_0 c_v}{1-\phi_0}\frac{\partial \mathbf{v}_1}{\partial t} = \\ = -\mathbf{i}\rho_f g - \beta_0(\mathbf{u}_1 - \mathbf{v}_1) - \mathbf{i}\beta_0' \phi_1 - \nabla p_1^f + \\ + \mu_0^f(\nabla^2 \mathbf{u}_1 + \frac{1}{3}\nabla(\nabla \cdot \mathbf{u}_1))\end{aligned} \tag{30}$$

$$\begin{aligned}\left[\rho_s \phi_0 + \frac{\rho_f \phi_0 c_v}{1-\phi_0}\right]\frac{\partial \mathrm{v}_1}{\partial t} - \rho_f \phi_0 \left[1 + \frac{c_v}{1-\phi_0}\right]\left(\frac{\partial \mathbf{u}_1}{\partial t} + u_0 \frac{\partial \mathbf{u}_1}{\partial t}\right) = \\ = -\mathbf{i}(\rho_s - \rho_f) g \phi_1 + \beta_0(\mathbf{u}_1 - \mathbf{v}_1) + \mathbf{i}u_0 \beta_0' \phi_1 - p_0^{s'} \nabla \phi_1 \\ + \mu_0^s(\nabla^2 \mathbf{v}_1 + \frac{1}{3}\nabla(\nabla \cdot \mathbf{v}_1))\end{aligned} \tag{31}$$

Here a suffix zero indicates that the term is evaluated at conditions corresponding to the base state and a prime denotes differentiation with respect to ϕ.

Equations (28)–(31) then form a set of eight linear partial differential equations in the six components of vectors $\mathbf{u}_1$ and $\mathbf{v}_1$ together with scalars ϕ_1 and p_1^f.

Solutions can be found by writing

$$(\mathbf{u}_1, \mathbf{v}_1, \phi_1, p_1) = (\hat{\mathbf{u}}_1, \hat{\mathbf{v}}_1, \hat{\phi}, \hat{p}_1^f) \exp(st) \exp((i\mathbf{k} \cdot \mathbf{x}) \tag{32}$$

where $\hat{\phi}_1, \hat{p}_1^f$ and the component $\hat{\mathbf{u}}_1, \hat{\mathbf{v}}_1$ are constants. Equations (28) to (30) then reduce to a set of eight linear algebraic equations with these as unknowns.

A nonvanishing solution exists only if the determinant of their coefficients vanishes, and this condition relates s to the vector $\mathbf{k}$. If the components of $\mathbf{k}$ are real these solutions represent travelling waves with the wave vector $\mathbf{k}$.

For each $\mathbf{k}$ the determinantal equation has eight roots, which will, in general, be complex numbers. Thus waves grow or decay as they propagate depending on the sign of the real part of s.

It is interesting evolution of perturbance ϕ_1. Taking the divergence of (30) and eliminating $\nabla \cdot \mathbf{u}_1$ and $\nabla \cdot \mathbf{u}_1$ from the result with the help of eq. (28) and (29) we find that

$$\frac{1}{\tau_0}\left[\frac{\partial \phi_1}{\partial t} + \mathrm{V}\frac{\partial \phi_1}{\partial x}\right] - \nu_e \frac{\partial}{\partial t}\nabla^2 \phi_1 + \frac{\partial^2 \phi_1}{\partial t^2} + c_1 \frac{\partial^2 \phi_1}{\partial x \partial t} + \\ + \frac{1}{2} c_1 \mathtt{u}_0 \frac{\partial^2 \phi_1}{\partial x^2} - \frac{p_0^{s'}}{A\rho_s}\nabla^2 \phi_1 = 0 \tag{33}$$

where the new coefficients introduced are given in Appendix.

Substituting a trial solution $\phi_1 = \hat{\phi_1} \exp(st) \exp(i\mathbf{k} \cdot \mathbf{x})$ into (33) leads quadratic equation relating s to $\mathbf{k}$, since (33) is second order in time.

The two roots of this equation then yield nonvanishing solution for ϕ_1. The remaining six roots of the determinantal equation must, therefore belong to solution for which $\phi_1 = 0$. But then it follows from equation (28) and (29) that $\nabla \cdot \mathbf{u}_1 = \\ = \nabla \cdot \mathbf{v}_1 = 0$ and consequently $\mathbf{k} \cdot \mathbf{u}_1 = \mathbf{k} \cdot \mathbf{v}_1 = 0$. Thus there solution are tranverse waves that generate no disturbances of particle concentration.

We shall not study these but will confine our attention to the solution of (33) which should be visible as waves of varying particle concentration.

It is useful to rewrite (33) in dimensionless form. There are several different choices for the length and time scales needs to do this. For the purpose of stability theory the equations are reduced to their simplest form if dimensionless Cartesian coordinates and a dimensionless time are define by

$$(\chi, \eta, \zeta) = \frac{(x, y, z)}{\sqrt{\nu_e \tau_0}}, \quad \tau = \frac{\mathrm{V}}{\sqrt{\nu_e \tau_0}} \tag{$*$}$$

We seek a solution of equation (33) after transformation $(*)$ in the form of plane waves with vector k:

$$\phi_1 = \hat{\phi}_1 \exp(\boldsymbol{\sigma}\tau) \exp(i\mathbf{k} \cdot \chi) \tag{34}$$

where $\chi = (\chi, \eta, \zeta)$. Then $\boldsymbol{\sigma}$ must satisfy the following quadratic equation that in compact form one can to write:

$$\boldsymbol{\sigma}^2 + (p + iq)\boldsymbol{\sigma} + P + iQ = 0 \tag{35}$$

where

$$p = (1 + k^2)\upsilon/\mathrm{V} \quad q = \cos\theta k c_1/\mathrm{V} \\ P = (d - e\cos^2\theta)k^2/\mathrm{V}^2 \quad Q = \cos\theta k \upsilon/\mathrm{V} \tag{36}$$

with

$$d = p_0^{s'}/A\rho_s \quad \text{and} \quad e = \frac{1}{2}c_1 u_0, \quad k = |\mathbf{k}| \quad \text{and} \quad \theta$$

denotes angle subtended between the vector **k** and upward vertical direction. In direction of versor **i**. The roots of equation (35) are given by

$$2\boldsymbol{\sigma} = -(p + iq) \pm \sqrt{(p^2 - q^2 - 4P) + i(2pq - 4Q)} \tag{37}$$

and the root of interest here is that with larger real part. Its real and imaginary parts are given by

$$\alpha = Re(\boldsymbol{\sigma}) = \frac{1}{2}[M - p] \quad Jm(\boldsymbol{\sigma}) = \frac{1}{2}[N - q] \tag{38}$$

where

$$M = \left(\frac{\sqrt{a^2 + b^2} + a}{2}\right)^{1/2}, \quad N = sgn(b)\left(\frac{\sqrt{a^2 + b^2} - a}{2}\right)^{1/2} \tag{39}$$

with the positive value taken for each square root, and

$$a = p^2 - q^2 - 4P \qquad b = 2pq - 4Q$$

using (36) these expressions become:

$$a = \left(\frac{\upsilon}{\mathrm{V}}\right)^2 (1 + k^2)^2 + \frac{k^2}{V^2}\left\{(2c_1 \mathrm{u}_0 - c_1^2)\cos^2\theta - 4d\right\} \tag{40}$$

$$b = 2k\frac{\upsilon}{\mathrm{V}}\left\{(1 + k)\frac{c_1}{\mathrm{V}} - 2\right\}\cos\theta \tag{41}$$

Equations (38)–(41) provide a prescription for computing the dimensionless growth rate $\alpha(= Re\boldsymbol{\sigma})$ and velocity of propagation $v(= -Jm(\boldsymbol{\sigma})/k)$ for a small-amplitude disturbance wave with any specific wave vector **k**. These functions $\alpha(k, \theta)$ and $v = v(k, \theta)$ are referred to as the dispersion relations for small disturbances.

Jackson examine form of this function in some detail. We are limited to a few remarks. Point of depart at first equation (33) and simple observe character of dependence of the growth rate of α on the angle θ, for given values **k** and the other parameters of the system. Since p is independent of θ the first of equation (38) shows that α is monotone for M. $M > 0$ and M is largest, when M^2 is largest. Thus α is largest at the value of θ that maximizes of M^2.

But from (39)

$$2\frac{d(M^2)}{d\theta} = \left(1 + \frac{a}{\sqrt{a^2 + b^2}}\right)\frac{da}{d\theta} + \frac{b}{\sqrt{a^2 + b^2}}\frac{db}{d\theta}$$

and after simple consideration we have conclusion, $\dfrac{d(M)^2}{d\theta} < 0 \quad$ for $0 < \theta < \frac{\pi}{2}$ showing that M, and hance α is largest when $\theta = 0$. Thus for any given value k the growth rate is bigger for a disturbance that propagates in upward-vertical direction. It is well-known fact that the main instability lies in vertical direction. This result is consistent with those of Göz (1992) [17].

Thus we may, therefore, limit attention to this vertical disturbances.

After a simple algebra we have inequality

$$d - \frac{1}{2}u_0 c_1 < -c_1^2/4 \tag{42}$$

It is sufficient condition for α to be positive for all values of k, in other wards, for disturbances of all wavelengths to grow

$$\alpha \approx k^2 \left[\frac{\mathrm{V}(\mathrm{V} + \frac{1}{2}u_0 c_1 - d}{v\mathrm{V}}\right], \quad v \to 1, \quad \text{as} \quad k \to 0 \tag{43}$$

All the above results can now be organized into a systematic description of the form of the function $\alpha(k)$ and how this changes as d is increased progressively from zero. They are four qualitatively distinct intervals, as follows:

a) $d - \frac{1}{2}u_0 c_1 < -c_1^2/4$,

b) $-\frac{c_1^2}{4} < d - \frac{1}{2}u_0 c_1 < 0$,

c) $0 < d - \frac{1}{2}u_0 c_1 < \mathrm{V}(\mathrm{V} - c_1)$,

d) $\mathrm{V}(\mathrm{V} - c_1) < d - \frac{1}{2}u_0 c_1$.

Instead of comments (it is very long) we presents illustrative figures. Figure 1(ii) to (vii). This shows α as a function k for a system with c_1/v=0,5, v/V=2 and successively increasing values of $(d - \frac{1}{2}u_0 c_1)$/V. Figures (ii) and (iii) belong to case a), (vi) belong to case c) and (vii) belong to case d).

Figure 1(vii) represents a stable case, where α decreases monotonically from zero as k increases. In all other figures there exist values of k for which α is positive, so the bed is unstable.

Jackson (2000)[23] propose the stability condition in form:

$$d - \frac{1}{2}u_0 c_1 > \mathrm{V}(\mathrm{V} - c_1) \tag{44}$$

or, put the value of d

$$\frac{p_0^{s'}}{A\rho_s} > V(V - c_1) + \frac{1}{2}u_0 c_1 \tag{45}$$

Inserting the values of $\mathbf{V}$ and c_1 (look Appendix) we can rewrite (44) in the following form:

$$\frac{p_0^{s'}}{\rho_s u_0^2} > n^2\phi_0^2 + \frac{\rho_f}{\rho_s}\frac{\phi_0}{1-\phi_0}\left\{(n\phi_0 - 1)^2 + c_v\left[1 + \frac{(n-1)^2\phi_0}{1-\phi_0}\right]\right\} \tag{46}$$

The possibility of securing of stable bed in this way, if the $p_0^{s'}$ must be sufficiently large was pointed out by Garg & Pritchett (1975) [12].

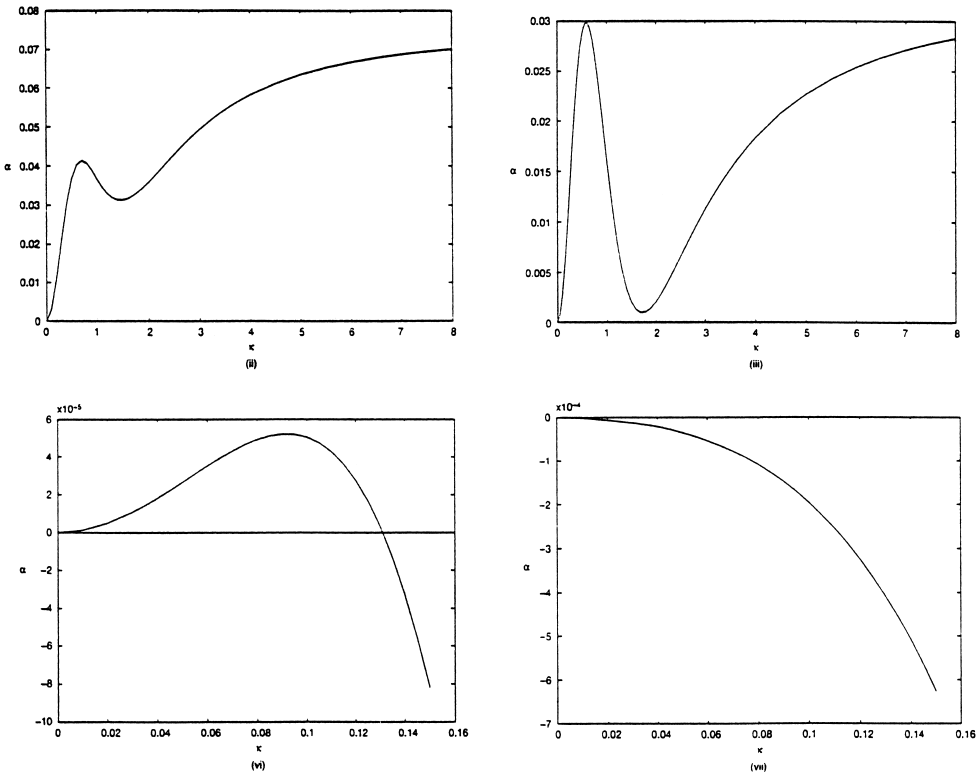

Fig. 1. Example of dispersion relation for the growth rate (From: Jackson (2000) [23]). $c_1/\mathrm{V} = 0.5$, $v/\mathrm{V} = 2$ in all cases. (ii) $(d - \frac{1}{2}u_0c_1)/\mathrm{V}^2 = -0.15$, (iii) $(d - \frac{1}{2}u_0c_1)/\mathrm{V}^2 = = -0.065$, (vi) $(d - \frac{1}{2}u_0c_1)/\mathrm{V}^2 = -475$, (vii) $(d - \frac{1}{2}u_0c_1)/\mathrm{V}^2 = 0.525$

The criteria of stability Foscolo & Gibilaro (1987) [10], Batchelor (1988) [4] and Jackson (2000) [23], inequality (44) in this revious, give conditions for growth or decay of very small amplitude disturbances of state of uniform fluidization, their success has been judged above on the basis of their agreement with observations of bubbling, which is a very large amplitude phenomenon. It cannot be emphasized too strongly that instability, implying that small disturbances will begin to grow necessarily continue to grow into anything resembling bubbles.

Problem of stability of dispersion flow (water drops in air was examined by Schulz in thesis (1979) [36] and (1985b) [37]. General result — the flow is unstable for each perturbation ϕ, (for $\phi \to 0$). Formally correspond with a case of Jackson. In reality it is difficult to compare this situation because in one equation of motion for liquid phase author was assumed $\mu_f = 0$ and drag force $\mathbf{F} = \alpha(\mathbf{u} - \mathbf{v})|\mathbf{u} - \mathbf{v}|$ (see (17)), ($Re \gg 1$). Jackson was assumed linear form drag force (7). Method of calculations in first etaps are similar.

5. THE CERTAIN RESULTS OF STABILITY OF FLUIDIZED BEDS USING COMPUTATIONAL METHOD

The analytical analysis of dispersion relations $\alpha = \alpha(k, \theta)$ and $v = v(k, \theta)$ is difficult because this functions are very complicated.

We discuss report Anderson *et al.* (1995) [3] exactly — this part of the paper dedicate to one-dimension case of flow.

As a basic state we denote that stationary and homogenous solutions of equations of motions for which particles do not move while the fluid is moving with constant velocity against the direction of gravity. This state is unique up to Gallilei transformations.

With the closures (8) (9) there is an equilibrium solution to (1)–(7) which represents uniform fluidized beds of infinite extent with

$$\phi = \phi_0; \quad \boldsymbol{v} = 0, \quad \mathbf{u} = \mathbf{i}u_0 = \mathbf{i}v_f(1-\phi_0)^{n-1}; \quad \nabla p_f = [\rho_s\phi + \rho_f(1-\phi)\mathbf{g}] \tag{47}$$

where $\mathbf{i}$ is the unit vector in the x-direction pointing vertically upward, and ϕ_0 and u_0 are constants.

When ϕ_0 is smaller than some critical values these solutions are linearly unstable to small spatially periodic disturbances.

The fastest growing disturbance is an upward travelling wave, of the form $\exp(\boldsymbol{\sigma}_r t)\exp[i(ky - \boldsymbol{\sigma}_i t)]$ whose wavefronts are horizontal planes.

The question of dependance and stability of solutions of equations (1)–(7) from parameters p, M, μ_s, μ_f, β, r, etc. was discussed in Section 2 et 3.

We seek solutions in a rectangular spatial domain of vertical height L_y and horizontal width L_x. The solutions will be constrained to be periodic with period L_y in the y-direction (except the pressure), and to be symmetric about the vertical median line (x=0) and periodic with period L_x in the x-direction. We can write explicite:

y-periodicity:

$$\phi(x,0) = \phi(x,L_y); \quad \mathbf{u}(x,0) = \mathbf{u}(x,L_y); \quad \boldsymbol{v}(x,0) = \boldsymbol{v}(x,L_y);$$

$$p(x,0) = p(x,L_y) + \Delta p \tag{48}$$

Symmetry and x-periodicity:

$$u_x = v_x = \frac{\partial \phi}{\partial x} = \frac{\partial u_y}{\partial x} = \frac{\partial v_y}{\partial x} = 0 \quad at \quad x = 0, \quad L_x/2 \tag{49}$$

Note that conditions (47) suppress any solutions in the form of oblique travelling waves. Because of symmetry about the median line the solution can be confirmed to the half-rectangle, and no conditions are needed at $x = -L_x/2$.

In (47) Δp denotes the change in pressure over the height of rectangle. Its value must be adjusted to ensure that average vertical solids flux vanishes in the

laboratory reference frame, thereby eliminating the inherent translational ambiguity of the problem.

These boundary conditions ensure that the total volume of each phase within the rectangle remains constans.

Difficult question of existence and uniquenes of solutions fluidized bed equations was briefly analized by Göz (1991) [16]. It was using Schauder fixed point theorem.

Anderson *et al.* not limit considerations to small perturbations of uniform state but they was generate the solutions by direct numerical integration of the full nonlinear equations of motions. The integration will always start from a small perturbation of a known steady state (its can be predicted from eigensolutions generated by the linearization about the base state).

The discretization was performed using Galerkin finite element method, with rectangular elements. For the fluid pressure billinear functions of coordinates within each element are used, and for the remaining variables biquadratic functions. The solutions is advanced in time using an implicid one-step Euler method. More numerical details and estimations see, f.e. Brenner & Scott (1991) [5].

The particular choice of characteristics length is motivated by the linear stability analysis of uniform state (see Liu (1982) [30]). For the purpose of computations it is clearly desirable to scale lengths in the specified size of periodic cell. Two other quantities are needed, to make the equations dimensionless. In gaz-fluidized bed solid mass is dominance and ρ_s is used for scale of mass.

The terminal velocity v_t is appropriate to chose for scaling the velocity (they are other possibility to do this) so that dimensionless variables are defined as follows:

$$x* = \frac{x}{L_x}; \quad y* = \frac{y}{L_y}; \quad t* = \frac{tv_t}{L_y}, \quad (u*, v*) = \frac{(u, v)}{v_t}, \quad (\boldsymbol{\sigma}_f*, \boldsymbol{\sigma}_s*) = \frac{(\boldsymbol{\sigma}_f, \boldsymbol{\sigma}_s)}{\rho_s v_t^2}.$$

Which introduces the following dimensionless parameters:

$$\rho_a v_t L_y/M, \quad P/\rho_s v_t^2, \quad v_t^2/\mathrm{g}L_y, \quad \rho_f/\rho_r, \quad \mu_f/M$$

in addition to the dimensionless parameters r and ϕ_p. The question of physically appropriate scaling for the problem of disturbance propagation in fluidized bed is a difficult on. At best, therefore, we must settle for scaling related to effective properties the uniform bed which are, in principle, independently measurable.

Two model systems in work Anderson *et al.* (and Glasser *et al.* 1996)[14] are comon, namely 200 μm diameter glass beads fluidized by air at ambient conditions and 1 mm diameter glass beads fluidized by water. Their properties are listed in Table 1.

With the expression analytical (8) or other for p_s there is further difficulty because p_s is not boundet when $\phi \to \phi_p$.

Table 1. Properties of the air-and water fluidized beds

	Air	Water
ρ_s	2.2 g cm^{-3}	2.2 g cm^{-3}
ρ_f	0.0013 g cm^{-3}	1 g cm^{-3}
μ	0.000181 g cm^{-1} s^{-1}	0.01 g cm^{-1} s^{-1}
a	100 μm	0.5 mm
v_t	142 cm s^{-1}	14.3 cm s^{-1}
n	4.25	3.65
ϕ_p	0.65	0.65
r	0.3	0.3
m	0.571 g cm^{-1}s	0.571 g cm^{-1}s
p	10.78 dyn cm^{-2}	0.266 dyn cm^{-2}

Anderson *et al.* sketched as broken curve in Figure 2. There is phenomenon of minimum of fluidization. The actual behaviour of beds like those treated in discussed work is represented better by a form for p_s indicated by the solid curve sketched in Figure 2. Then both p_s and its derivative with respect to ϕ remain bounded for all $\phi < \phi_p$. ϕ_c — denote critical value of ϕ where the uniform suspension becomes unstable. ϕ_c=0,578 (Anderson *et al.*)

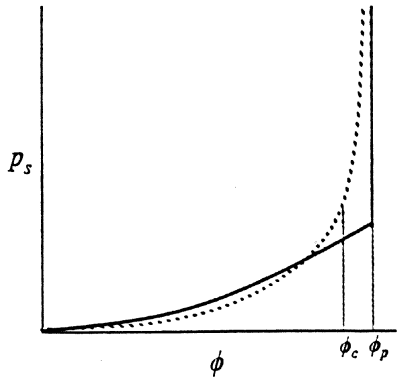

$$p_s = p\phi^3 \exp\left(\frac{r\phi}{\phi_p - \phi}\right)$$

Fig. 2. Dependence of p_s on ϕ in this work (broken curve) compared with *l*a more realistic form of this dependance (continous curve). (From Anderson *et al.* (1995) [3])

They fix the volume fraction of solids in the bed at value just below the critical value and examined instabilities and solutions for this case, the chosen value denoted by ϕ_o. It is ϕ_o=0.57. This is the base state for gas — and liquid bed. After linearization equations of motions one can found the growth σ_r, and velocity of propagation v, of small perturbations sinusoidal in y, in the uniform gas-fluidized bed (as a functions of wavenumber, k, both at the expansion corresponding to limiting stability, and at ϕ_o).

This is imagined on Figure 3(a) — the growth δ_r, and Figure 3(b) — the velocity of propagation v.

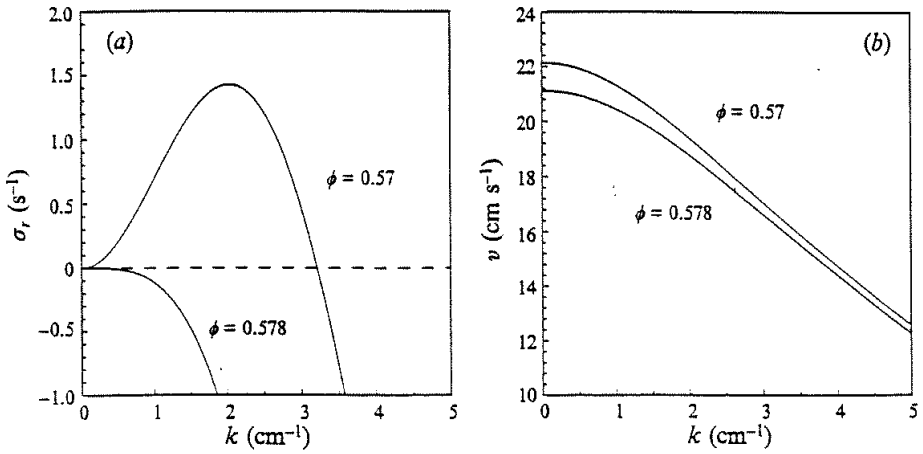

Fig. 3. Linear stability results for one-dimensional waves in air-fluidized bed of 200 μm glass beads: (a) growth rate σ_r, (b) wave speed v, as function of wavenumber k. (From Anderson *et al.* (1995) [3])

Figures 4(a) and (b) give the corresponding information for the water-fluidized bed, and here wave length of dominant disturbance is 1.86 cm.

In Table 2 are listed all properties of dominant small disturbance for each bed.

Table 2. Properties of the unperturbed uniform beds

	Gas	Liquid
Solid volume fraction, ϕ_0	0.57	0.57
Fluidized velocity, u_0	9.14 cm^{-1}	1.53 cm^{-1}
Continuity wave speed, V	22.15 cm s^{-1}	3.18 cm s^{-1}
Upward dynamic wave speed, c_u	16.57 cm s^{-1}	2.07 cm s^{-1}
Downward dynamic wave speed, c_d	16.55 cm s^{-1}	1.02 cm s^{-1}
Wavelength of dominant mode, λ^m	3.14 cm	1.86 cm
Speed of dominant mode, v^m	19.4 cm s^{-1}	2.82 cm s^{-1}
Growth time of dominant mode $1/\boldsymbol{\sigma}_r^m$	0.689 s	36.1 s

For definitions of the continuity and dynamic wave velocities see for example, Liu (1982) [30] and Kolev (2002) [27].

From Figure 4(a) it follow that there is a critical value of wavenumber for each bed, above which the uniform bed is stable, and this increases as bed is expanded. As a result computational elements become unstable.

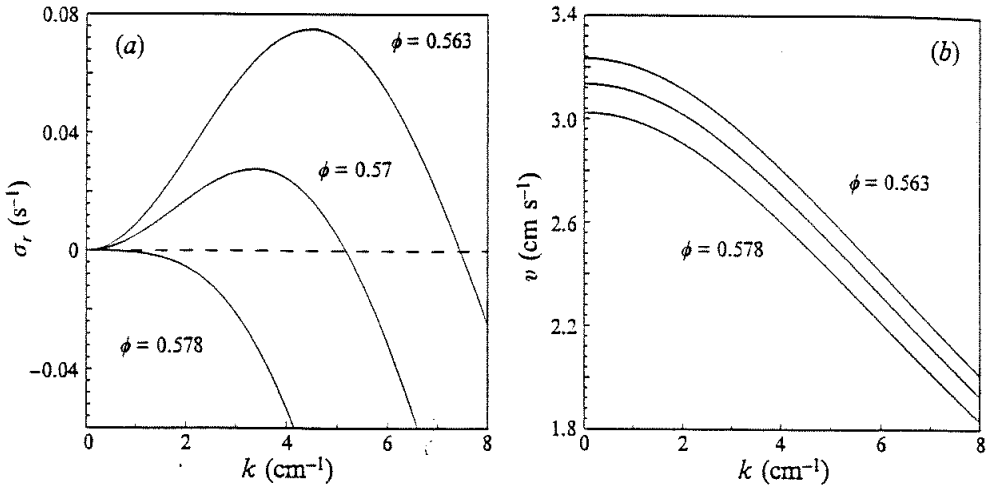

Fig. 4. Linear stability results for one-dimensional waves in a water-fluidized bed of 1 mm glass beads: (a) growth rate σ_r, (b) v, as funtion of wavenumber k. (From Anderson *et al.* (1995) [3])

5.1. ONE DIMENSIONAL STRUCTURES

Anderson *et al.* was considered the next problem the propagation and growth of one-dimensional waves with horizontal wavefronts. The initial stages of motion can than be found analytically by linearization about the uniform bed, introducing a perturbation of the form $\exp(\boldsymbol{\sigma}^* t^* + ik^* y^*)$ in terms of dimensionless variables used in the computations, where $\boldsymbol{\sigma}^* = \boldsymbol{\sigma}_r^* - i\boldsymbol{\sigma}_i^*$. This is valuable in a number of ways for the subsequent numerical integration.

Linear stability theory indicates only qualitative differences between gas- and liquid-fluidized beds, both growth rates and speeds of propagation being much larger in the former.

It is convenient to suppress the merely quantitative differences by scaling times in terms of growth of time $\left(\frac{1}{\sigma_r^m}\right)$ for the fastest grow in small perturbation. Lengths was scaled in terms of wavelength λ^m of this perturbation (= 3.14 cm). Determining these dimensions by tildes, we have

$$\tilde{t} = t\boldsymbol{\sigma}_r^m, \quad \tilde{L}_y = L_y/\lambda^m, \quad \tilde{v} = v/\mathrm{V}\sigma_r^m,$$

Computations was performed for gas-fluidized bed and cell with $L_y = \pi \approx 3.14$ cm (the wavelength λ^m of the dominant linear mode). Authors adopted algoritm for two-dimensional motions making the cell narrow in lateral direction and other modifications.

Convergence of computations was seen to be rapid the grid was rafined. With twenty intervals the real and imaginary parts of the dominant computed and expli-

citly determined eigenvalue differ by no more than one in the fourth significant figure. Figure 5(a) illustrates the computed development of initially small, sinusoidal perturbation with the wavelength $\lambda^m = 3.14$ cm 5(b) for $2\lambda^m$, 5(c) for $3\lambda^m$, respectively.

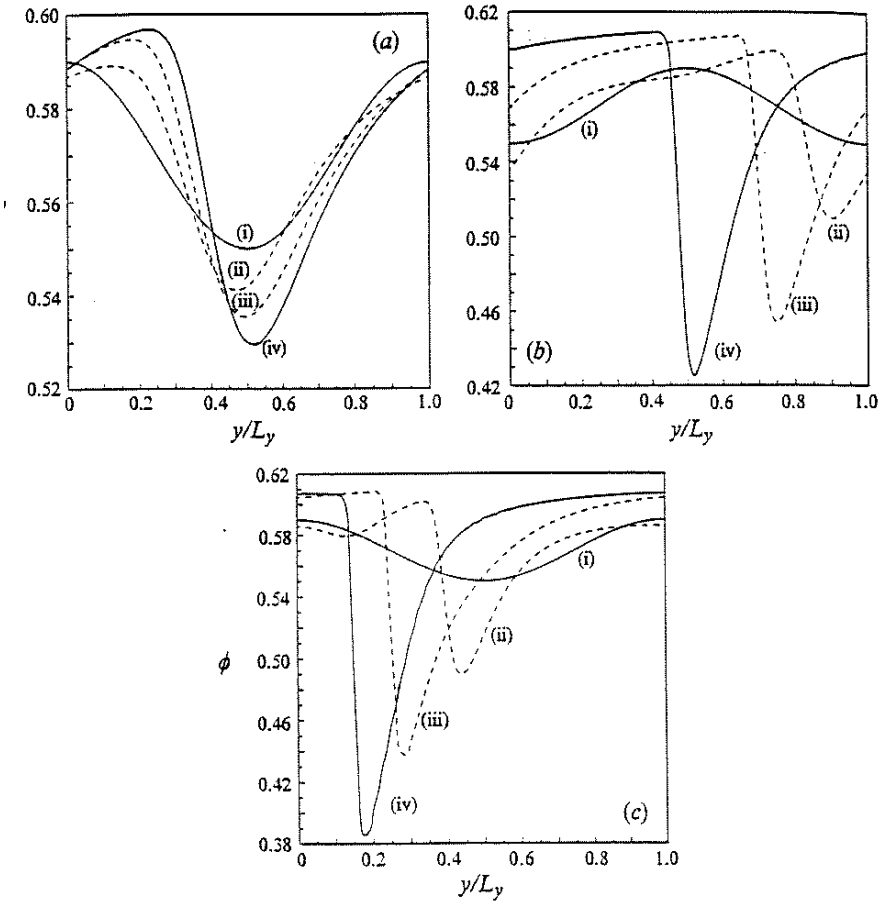

Fig. 5. Development of one-dimensional waves in the air-fluidized bed. The fastest growing wave $\tilde{L_y} = 1$: $\tilde{t} = 0$, $(ii) = 0$. $\tilde{t} = 0.16$: (iii) $\tilde{t} = 0.80$, (iv) $\tilde{t} = 2.9$; initial wave speed: $\tilde{v} = 0.876$ final wave speed: $\tilde{v} = 0.8444$. (b) $\tilde{L_y} = 2$: (i) $\tilde{t} = 0$, (ii) $\tilde{t} = 0.58$, (iii) $\tilde{t} = 2.58$, (iv) $\tilde{t} = 2.85$; initial wave speed $\tilde{v} = 0.9666$ final wave speed: $\tilde{v} = 0.862$ (c) $\tilde{L_y} = 3$: (i) $\tilde{t} = 0$, (ii)$\tilde{t} = 0.97$, (iii) $\tilde{t} = 2.58$, (iv) $\tilde{t} = 2.85$; initial wave speed: $\tilde{v} = 0.975$, final wave speed: $\tilde{v} = 0.889$. (From Anderson *et al.* (1995) [3])

No significance should be attached to the relative horizontal displacements of the profiles; they are arbitrary do not indicate displacement of the profiles in times (the reference frames was changed from time to time. See also Glasser *et al.* (1996) [14]).

With increase in wavelength the most striking change is the marked increase in depth of band of low concentration particles.

We can discuss case from Figure 5(c). Other are similar. Profiles from Figure 5(c) start from the low-amplitude sinusoidal wave labelled (i) end with a profile labelled (iv) that is no longer changing significantly and can therefore be assumed to be a good approximation to the fully developed wave. The amplitude of this fully developed wave is ≈ 0.22 and there is a very marked asymmetry, indeed the periodic wave now consists of sequence of plugs densely packed particles, with ϕ remains near 0.6, separated by relatively narrow bands of significantly lower density. The upper surface of each plug is quite sharp but its lower boundary is diffuse as the density decreases gradually to a minimum value. This type of motion is commonly observed in practice in gas fluidized beds contained in narrow tubes. The lower end of each plug is unstable and diffuses (erodes), giving rise to a region of gradually falling density as the particles rain accelerate downward under gravity. These falling particles are then decelerated suddenly when they meet the sharp upper boundary of the plug below, and their transfer from the lower surface of one plug to upper surface of the plug below is responsible for the upward movement of whole concentration pattern.

This asymmetry has previously been predicted, on different grounds, by Fanucci *et al.* (1981) [9], Ganser & Drew (1990) [6], Göz (1992) [17] and Glasser *et al.* (1997) [28], Lammers & Biesheuvel (1996) [29]; Joseph (1993) [24]. A problem of dispersion flow of water drops in stream of air in very long tubes (mine ventilation shaft) was analysed by Schulz (1979) [36] and (1985) [37]. In first work on can find sidenote — hipotesis: in the ventilation shaft of mine in which to appear suspension of water drops uniform state is rarely realized in practice and becomes unstable and suspension form periodic plugs of high concentration of drops and zones of low concentration keeping balance dynamic in motion. In non favorable condition, perturbation of this equilibrium hierarchy one can put in motion the 'machinery' of cascade: the plug number n_0 break 'down' on plug $n_0 - 1$, this on $n - 2$, etc.

1° If resistance of flow increase — this can interrupt process and return to l equlibrium.

2° Continuation. In result global loss of stability and even revers of flow l in ventilation shaft including. (It is possible finish catastrophe like l in the mine "Arenberg" in R.F.N.) This hypothesis correspond with l analogous thesis in work Anderson *et al.* (1995) [3] (comment to l l Fig. 5c)), and Glasser *et al.* (1997) [15]. On can say that this l l researchers by direct computing attest this hypothesis in laboratory l situation (tout proportion gardé).

Figure 6 is similar to Figure 5(c) but shows the evolution of one-dimensional waves from small initial perturbation of the water-fluidized bed. The wavelength λ^m (= 1.86 cm) corresponds to the fastest growing small perturbation, while Figure 6 exhibit $3\lambda^m$. Note that the speed the fully developed wave is somewhat smaller than that of the initial small-amplitude wave in the air fluidized system.

The only noticeable qualitative difference between the gas-and liquid-fluidized systems lies in the asymmetry of the particle concentration profiles which is less marked for the liquid-fluidized bed.

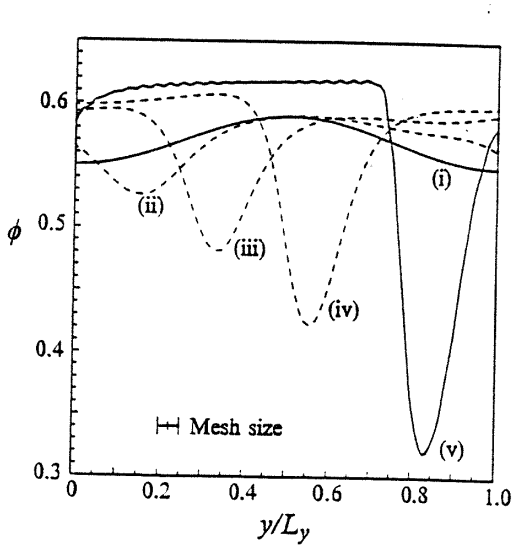

Fig. 6. Development of one-dimensional waves in the water-fluidized bed $\tilde{L}_y = 3$: (i) $\tilde{t} = 0$, (ii) $\tilde{t} = 0.64$ (iii) $\tilde{t} = 1.20$ (iv) $\tilde{t} = 1.52$, (v) $\tilde{t} = 2,16$; initial wave speed: $\tilde{v} = 0.975$, final wave speed: $\tilde{v} = 0.984$

There is no qualitative distinction in behaviour that could explain why bubbles are seen, in practice, in the gas-fluidized case, but not in the liquid-fluidized case. Thus, this problem is not resolved by replacing a linear small-amplitude approximation by the full nonlinear equations if considerations remains within the framework one-dimensional motions.

Stability of the fully developed one-dimensional waves.

1° Observed from a frame of reference moving at its own speed, a fully developed wave is a time-independent solution of the equation of motion. Its stability can be investigated either by retaining the constraint of one-dimensionality, or by viewing it as a degenerate case of a two-dimensionality, or by viewing it as a degenerate case of a two-dimensional solution and questioning its stability to two-dimensional perturbations. Anderson *et al.* have been computed each of the fully developed waves described in the previous section is founded to have only eigenvalues with negative real parts, provided the perturbed wave is constrained to remain one-dimensional and to retain the same minimum spatial period as the fully developed wave itself.

With these constraints, all the fully developed, one-dimensional waves reported here are stable.

2° Each fully developed solution is also periodic with any integer multiple of its shortest period.

Each wave is stable to perturbations constrained to its smallest period, but unstable when the constraint is relaxed to a multiple of this period. When this multiple is twice the smallest period, adjacent bands od low particle concentration caolescence, leading to the fully developed wave with wavelength twice that the original wave.

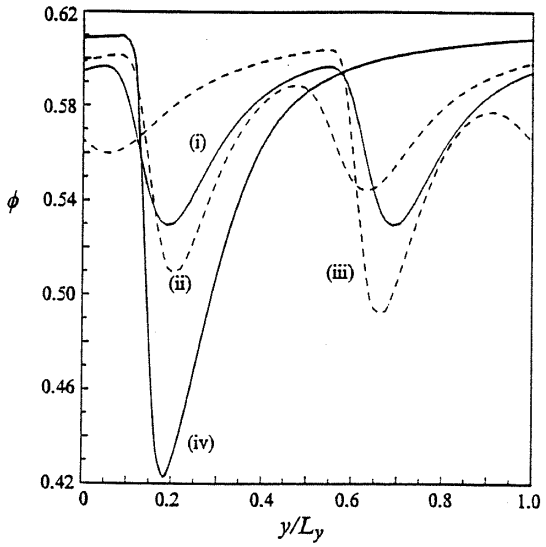

Fig. 7. Coalescence of adjacent waves of the fully developed one-dimensional wavetrain of wavelength λ^m in the air-fluidized bed, when constrained to cell with $L_y = 2\lambda^m$. (i) $\tilde{t} = 0$, (ii) $\tilde{t} = 3.19$, (iii) $\tilde{t} = 5.81$, (iv) $\tilde{t} = 9.0$. Final wave speed: $\tilde{v} = 0.862$. From Anderson *et al.* (1995) [3]

After perturbing the fully developed wave by adding a small multiple of the corresponding eigenfunction, numerical integration generates the sequence of concentration profiles shown in Figure 7.

5.2. CONCLUSION

Anderson *et al.* (1995) [3] have been examined the growth of one-end two-dimensional (non presented here) structures in bubbling and non bubbling systems through transient integration of averaged equations of motions assuming spatial periodicity.

They have established that the existence of bubble-like solutions for gas fluidized bed is a robust phenomenon, independent of the specific closures used to describe the particle-phase pressure and viscosity. Apparently stable bubble-like solutions evolved smoothly in bed of glass beads fluidized by air.

In contrast, no such structures developed in bed of glass beads fluidized by water.

They went to conclude that eq. of motions with simple and credible closure relations contained the essential physics needed to distinguish between bubbling and non bubbling systems.

APPENDIX

A)

Table 3. Typical values for Reynolds and Stockes numbers

	ε	
d	0.5	1.0
50 μm	$Re = 0.045$	$Re = 0.50$
	$St = 74.3$	$St = 832$
200 μm	$Re = 2.75$	$Re = 22.1$
	$St = 4587$	$St = 36.796$
1 mm	$Re = 130$	$Re = 417$
	$St = 217.211$	$St = 694.555$

B) Coefficients for eq. (33)

$$A = 1 + \frac{\rho_f}{\rho_s}\frac{\phi_0}{1-\phi_0}\left(1 + \frac{c_v}{\phi_0(1-\phi_0)}\right)$$

$$\tau_0 = \frac{A\rho_s\phi_0(1-\phi_0)}{\beta_0} = \frac{A(1-\phi_0)u_0}{(1-\rho_f/\rho_s)g}$$

$$\nu_e = \frac{4\mu_0^s/3}{A\phi_0\rho_s}$$

$$\mathrm{V} = u_0\left[2\phi_0 - 1 + \frac{\phi_0(1-\phi_0)\beta_0'}{\beta_0}\right] = n\phi_0 u_0$$

$$c_1 = \frac{2u_0}{A}\frac{\rho_f}{\rho_s}\frac{\phi_0}{1-\phi_0}\left(1 + \frac{c_v}{1-\phi_0}\right)$$

(for particles with $\rho_s = 2.2$).

(From Jackson (2000) [23])

REFERENCES

[1] Anderson T. B., Jackson, R.: *Fluid mechanical description of fluid beds. Equation of motion*. Ind. Eng. Chem Fundam. **7** (1967), 17–21.

[2] Anderson T. B., Jackson R.: *Fluid mechanical description of fluid beds. Comparison of theory and experiment*. Ind. Eng. Chem Fundam. **8** (1969), 137–144.

[3] Anderson K., Sundareson S., Jackson R.: *Instabilities and the formation of bubbles in fluidized beds*. J. Fluid Mech. **303** (1995), 327–366.

[4] Batchelor G. K.: *A new theory of instability of fluidized bed*. J. Fluid Mech. **193** (1988), 75–110.

[5] Brenner S. C., Scott L. T.: *The Mathematical Theory of Finite Element Methods*. Springer-Verlag, 1994.

[6] Drew D. A., Lahey R. T. Jr.: *Analytical modeling muliphase flow*. [in:] Particulare Two-Phase Flow, M. C. Roco (Ed.), Butterworth-Heinemann, 1993, pp. 510–566.

[7] Duru P., Nicolas M., Hinch J., Guzzelli É.: *Constitutive laws in liquid-fluidized beds*. J. Fluid Mech. **452** (2002), 371–404.

[8] El-Kaissy M. M., Homsy G. M.: *Instability waves and the origin of bubbles in fluidized beds*. Intl. J. Multiphasic Flow **2** (1976), 379–395.

[9] Fanucci J. B., Ness N., Yen R.-H.: *Structure of shock waves is gas particulate bed model*. Phys. Fluids **24** (1981), 1944–1954.

[10] Foscolo P. U., Gibilaro L. G.: *Fluid dynamic stability of fluidized suspension, the particle bed model*. Chem. Eng. Sci. **421** (1987), 1489–1500.

[11] Ganser G. H., Drew D. H.: *Nonlinear stability analysis of uniform fluidized bed*. Intl. J. Multiphase Flow **16** (1990), 447–460.

[12] Garg S., Pritchett J. W.: *Dynamics of gas-fluidized beds*. J. Appl. Phys. **46** (1975), 4499–4520.

[13] Gidaspow D.: *Multiphase Flow and Fluidization Continuum and Kinetic Theory Description*. Academic Press, 1994.

[14] Glasser B. I., Kevrekidis, Sundaresan S.: *One-and two-dimensional travelling wave solutions in gas-fluidized beds*. J. Fluid Mech. **306** (1996), 183–221.

[15] Glasser B. I., Kevrekidis & Sundaresan S.: *Fully developed travelling wave solution and bubble formation in fluidized beds*. J. Fluid Mech. **334** (1997), 157–188.

[16] Göz M. F.: *Existence and uniqueness of time-dependent spatially periodic solution of fluidized bed equations*. ZAMM 71 N^o T750-T751 (1991).

[17] Göz M. F.: *On the origin of the wave patterns in fluidized beds*. J. Fluid Mech. **240** (1992), 379–404.

[18] Göz M. F.: *Bifurcation of plane voidage waves in fluidized beds*. Physica D **65** (1993), 319–351.

[19] Göz M. F.: *Tranverse instability of plane wave trains in gas-fluidized beds*. J. Fluid Mech. **303** (1995), 55–81.

[20] Hu H., Crochet H. J., Joseph D. D.: *Direct simulation of fluid particle motion*. Univ. of Minnesota, Supercomputer Inst. Res. Rep. UMSI **91/190** (1991).

[21] Jackson R.: *The mechanics of fluidized beds.* Part I: *The stability of the state of uniform fluidization.* Trans. Inst. Chem. Engrs. **4** (1963).

[22] Jackson R.: *The mechanics of fluidized beds.* Part II: *The motion of fully developed bubbles.* Trans. Inst. Chem. Engrs. **41** (1963), 22–28.

[23] Jackson R.: *The Dynamics of Fluidized Particles.* Cambridge University Press 2000.

[24] Joseph D. D., Lundgren T. S.: *Finite size effect in fluidized suspension experiments in "Particulate Two Phase Flow".* [in:] Roco M.C., Butterworth-Heinemann 1993, 300–323.

[25] Joseph D. D., Lundgren T. S.: *Ensemble average mixture theory equation for incompressible fluid particle suspensions.* I.J. Multiphase Flow v. 16 n^{o}1 (1999), 35–42.

[26] Koch D., Sangani A. S.: *Particle pressure and marginal stability limits for a homogeneous monodisperse gas-fluidized bed: kinetic theory and numerical simulation.* J. Fluid Mech. **400** (1999), 229–263.

[27] Kolev M. I.: *Multiphase Flow Dynamic 1. Fundamentals* (2002).

[28] Kolev M. I.: *Multiphase Flow Dynamic 2. Termal and Mechanical Interactions* (+CD) Springer V. 2002.

[29] Lammers J. H., Bieheuvel A.: *Concentration waves and the instability of bubbly flows.* J. Fluid Mech. **328** (1996), 67–93.

[30] Liu J. T. C.: *Note on a wave-hierarchy interpretation of fluidized bed instabilities.* Proc. R. Soc. Lond. A. **380** (1982), 229–239.

[31] Murray J. D.: *On the mathematics of fluidization.* J. Fluid Mech. **21** (1965), 465–493.

[32] Needham D. J., Pritchett J. W.: *Dynamics of gas-fluidized beds.* J. Appl. Phys. **46** (1975), 4493–4500.

[33] Needham D. J., Merkin J. H.: *The existence and stability of quasi steady periodic voidage waves in fluidized.* Z. Angew. Mathem. Phys. **18** (1986), 119–132 ZAMP.

[34] Nigmatulin R. J.: *Spatial averaging mechanics of heterogeneous dispersed systems.* Intl. J. Multiphas. Flow **5** (1979), 353–385.

[35] Saurel R., Lemetayer O.: *A multiphase model for compressible flow with interfaces, shocs, detonation, waves and cavitation.* J. Fluid Mech. **431** (2001), 239–271.

[36] Schulz P.: *The continuous model of suspension flow in a mine ventilation shaft.* Kraków, IMG PAN 1979.

[37] Schulz P.: *On a problem of the so-called "water-lock rupture" in a mine ventilation shaft. P. I. General remarks. P. II. Stability of suspension flow.* Archiwum Górnictwa, t. 30, z. 2, 1985, pp. 225–234–241.

[38] Zhang D.Z., Prosperetti H.: *Averaged equations for inviscid disperse two-phase flow.* J. Fluid Mech. 267 (1994), 185–219.

Piotr Schulz

AGH University of Science and Technology
Faculty of Applied Mathematics
al. Mickiewicza 30, 30-059 Cracow, Poland

Received: December 19, 2003.